Aerosol Science and Technology

ISSN: 0278-6826 (Print) 1521-7388 (Online) Journal homepage: http://www.tandfonline.com/loi/uast20

Seasonal and Spatial Coarse Particle Elemental Concentrations in the Los Angeles Area

Payam Pakbin , Zhi Ning , Martin M. Shafer , James J. Schauer & Constantinos Sioutas

To cite this article: Payam Pakbin , Zhi Ning , Martin M. Shafer , James J. Schauer & Constantinos Sioutas (2011) Seasonal and Spatial Coarse Particle Elemental Concentrations in the Los Angeles Area, Aerosol Science and Technology, 45:8, 949-963, DOI: 10.1080/02786826.2011.571309

To link to this article: http://dx.doi.org/10.1080/02786826.2011.571309

View supplementary material

Published online: 13 Apr 2011.

Submit your article to this journal

Article views: 601

View related articles

Citing articles: 27 View citing articles

Full Terms & Conditions of access and use can be found at
http://www.tandfonline.com/action/journalInformation?journalCode=uast20

Download by: [University of North Texas] **Date:** 14 January 2017, At: 04:47

Aerosol Science and Technology, 45:949–963, 2011
Copyright © American Association for Aerosol Research
ISSN: 0278-6826 print / 1521-7388 online
DOI: 10.1080/02786826.2011.571309

Seasonal and Spatial Coarse Particle Elemental Concentrations in the Los Angeles Area

Payam Pakbin,[1] Zhi Ning,[1] Martin M. Shafer,[2] James J. Schauer,[2] and Constantinos Sioutas[1]

[1]*Department of Civil and Environmental Engineering, University of Southern California, Los Angeles, California, USA*

[2]*Environmental Chemistry and Technology Program, University of Wisconsin–Madison, Madison, Wisconsin, USA*

The concentrations of trace metals and elements in the coarse fraction of atmospheric particulate matter (CPM, particles smaller than 10 and larger than 2.5 μm in diameter, $PM_{10-2.5}$) and their spatial and temporal trends were investigated in the greater Los Angeles area. Ten distinct sampling sites were chosen to encompass a variety of CPM sources, including urban, rural, coastal, inland, and near-freeway sites. Time-integrated 24-h CPM samples were collected at each location once a week, for an entire year, from April 2008 to March 2009, to characterize drivers of the seasonal and spatial patterns of the CPM trace metal content. Metals were quantified using sector-field inductively coupled plasma mass spectrometry (SF-ICP-MS).

Trace metals in CPM displayed distinct seasonal and temporal variations, and a principal component analysis (PCA) was performed to aid the identification of the CPM sources underlying these variations. The probable sources of each principal component were identified using elemental tracers. Major sources of CPM metals and elements identified were crustal and mineral matter, abrasive vehicular emissions, industrial, sea spray, and catalytic converters, explaining more than 80% of the total variance of CPM metal content. Mineral and crustal elements, most notably Fe, Ca, Al, Mg, K, Ti, and Mn, were the main contributors to the overall CPM mass, accounting for over 33% of the total variance, followed by abrasive vehicular markers such as Cu, Ba, and Sb, accounting for over 16% of the variance, with an increasing contribution in the urban sites. Temporal and spatial variations in each identified class of CPM sources were also investigated.

[Supplementary materials are available for this article. Go to the publisher's online edition of *Aerosol Science and Technology* to view the free supplementary files.]

Received 22 October 2010; accepted 25 February 2011.

This research was supported by the US Environmental Protection Agency (EPA) under STAR grant no. RD833743 and MESA Air grant no. RD831697. We acknowledge the assistance of the Antelope Valley Air Quality Management District, the South Coast Air Quality Management District, and the USC Aerosol Laboratory group's current and previous members, Dr. A. Polidori, Dr. K. F. Moore, Dr. M. Arhami, V. Verma, N. Hudda, K. L. Cheung, for their participation in this project. This manuscript has not been subjected to the EPA's peer and policy review and therefore does not necessarily reflect the views of EPA agency.

Address correspondence to Constantinos Sioutas, Department of Civil and Environmental Engineering, University of Southern California, 3620 S. Vermont Ave., KAP210, Los Angeles, California, 90089 USA. E-mail: sioutas@usc.edu

1. INTRODUCTION

An extensive literature has demonstrated associations between exposure to inhalable particulate matter (PM), both $PM_{2.5}$ and PM_{10}, and a variety of acute and chronic health outcomes, including both respiratory and cardiac diseases (Hornberg et al. 1998; Monn and Becker 1999; Kleinman et al. 2003; Villeneuve et al. 2003; Becker et al. 2005; Lipsett et al. 2006; Yeatts et al. 2007). Studies suggest that the PM size is an important factor influencing aerosol toxicity; however, it is still unclear whether toxic PM properties are concentrated in a particular size range. Current PM emission regulations, which focus on mass emissions of $PM_{2.5}$ and PM_{10}, have several caveats. PM_{10} includes particles in both the $PM_{2.5}$ range as well as coarse PM (CPM—particles between 2.5 and 10 μm in aerodynamic diameter), and these size fractions can have substantially different sources, thus different chemical composition and as a result may lead to potentially different health outcomes (Pakbin et al. 2010). Most $PM_{2.5}$ particles are produced by combustion processes, whereas airborne coarse particles are generally the products of fugitive soil and dust. Nontailpipe emissions from traffic-induced resuspension of road dust can be as significant as primary exhaust emissions (Harrison et al. 2001). Moreover, an increasing number of studies have reported associations between adverse health effects and specific PM chemical classes or species, rather than total PM mass (Tsai et al. 2000; Claiborn et al. 2002). Among these compounds, trace element and metal species have been linked to various health impacts (Gavett

and Koren 2001; Luttinger and Wilson 2003). A number of studies suggest that the biochemical activity of certain metals and trace elements can contribute to the toxic properties of particles (Smith and Aust 1997; Lighty et al. 2000). Among the trace metal species, only arsenic (As), beryllium (Be), cadmium (Cd), cobalt (Co), chromium (Cr), mercury (Hg), manganese (Mn), nickel (Ni), lead (Pb), antimony (Sb), and selenium (Se) are listed by the US Environmental Protection Agency (EPA) as air toxics; however, various studies have linked many other trace metals to adverse health outcomes.

Nonexhaust roadway PM emissions are the result of resuspension of road dust, deposited from multiple sources, such as windblown soil, abrasion of road surface, wear of tires and brake linings, and from dry deposition of ambient PM, including those directly emitted from vehicular exhaust (Thorpe and Harrison 2008). Although road dust is primarily composed of mineral material (most commonly Al, Ca, K, Ti, etc.), it is also enriched in heavy metals and metalloids (Amato et al. 2009). Wear of brake lining and tire wear contribute greatly to the high metal content of particles, especially those in the CPM mode. Barium (Ba), copper (Cu), and zinc (Zn) are commonly used in brake linings as friction agents, while Mo, Sb, Sn, and sulfides are added as lubricants (Garg et al. 2000; Chan and Stachowiak 2004; Iijima et al. 2007). Vehicle exhaust catalytic converters are the main emission source of platinum group elements (PGEs; Rh, Pd, Pt) in the urban atmosphere, resulting from the mechanical stress on catalytic converters. Other elements such as Ce, La, Mo, and Ni are also commonly employed in catalytic converters (Gandhi et al. 2003; Morcelli et al. 2005; Colombo et al. 2008). Furthermore, the analysis of PM elemental composition, in addition to the evaluation of its impact on human health, can be used in the identification of specific emission sources (Querol et al. 2007; Canepari et al. 2009).

The goal of this study was to provide a database of the trace element and metal content of CPM in the greater Los Angeles area. The CPM samples were collected at 10 sites in distinctly different regions of the greater Los Angeles area, encompassing urban, rural–agricultural, industrial, coastal, and background desert sites, and affected by a variety of PM sources. Sampling was conducted once a week, for an entire year, to cover the seasonal variations at all the sites. Concentrations of forty-nine trace elements were quantified by sector-field inductively coupled plasma mass spectrometry (SF-ICP-MS) and principal component analysis (PCA) was employed to help identify their emission sources.

2. METHODOLOGY

2.1. Sample Collection

Ambient CPM samples were collected once a week from April 2008 to March 2009 at 10 sites in the greater Los Angeles area to capture the spatial and temporal variations in CPM constituents. Time-integrated 24-h samples were obtained from 12:00 AM PST to 11:59 PM PST on a weekday. Samples were collected using personal cascade impactor samplers (Sioutas PCIS, SKC, Inc., Eighty Four, PA, USA), at an air flow rate of 9 liters per min (LPM). Particles larger than 2.5 μm are impacted on Zefluor (25 mm, Zefluor, 0.5-μm pore size, Pall Corp., East Hills, NY, USA) after passage through a commercially available inlet designed to achieve the PM_{10} cut point (Misra et al. 2002, 2003; Singh et al. 2003). All the filter substrates were weighed before and after sampling, in the laboratory under controlled conditions, to determine the collected CPM mass. All filters were conditioned for 24 h in a room with controlled temperature (21°C ± 2°C) and relative humidity (30% ± 5%) before being weighed using a microbalance (Model MT5, Mettler-Toledo, Inc., Highstown, NJ, USA). Additional details of the sample collection protocols may be found in Pakbin et al. (2010).

2.2. Site Selection

Sampling sites were chosen to encompass the diversity of CPM sources and sinks in the greater Los Angeles area. The 10 selected sites (Table 1 and Figure S1 in the online supplemental information) include urban sites near freeways, residential sites located some distance from freeways, semirural, and desert sites. Table 1 summarizes the relevant information about each site, including sampling region, designation code, description, geographic coordinates, and data recovery. The sites are categorized geographically into eastern, central, and western Los Angeles; Riverside County; Long Beach; and Lancaster. A detailed description of each site has been reported previously by Pakbin et al. (2010). In brief, sampling sites located in the urban regions of Los Angeles were segregated into three regions: eastern, central, and western Los Angeles. Eastern Los Angeles sites—HMS and FRE—and the centrally located USC and CCL sites were in close proximity to a network of major freeways, east and south of downtown Los Angeles respectively, while the western Los Angeles sites—LDS and GRD—can be classified as coastal sites, although both sites were also close to major roadways.

Riverside sites—GRA and VBR—were located 80 km inland from downtown Los Angeles, in residential areas with a semirural nature. Both sites were adjacent to major roadways; however, GRA was located immediately (300 m) north of the CA-60 freeway and therefore it may be impacted to a greater extent by freeway traffic. The Long Beach site—HUD—was located immediately to the east of the Terminal Island Freeway (SR-103) and close to the I-710 freeway, both of which have a high fraction and volume of heavy duty diesel vehicle traffic. HUD was also directly affected by the ports of Los Angeles and Long Beach activities. In contrast, the desert site (LAN) was in desert-dominated Antelope Valley, north of the Los Angeles Basin (LAB), and over 2 km away from the nearest freeway, although in the proximity of locally significant surface arterial roadways. More details on each site and the general meteorology of the various regions are described in Pakbin et al. (2010). The VBR, HUD, and LAN sampling sites are also part of the Air Quality Management District (AQMD) monitoring network.

TABLE 1
Site information including sampling area, the designation code, description, geographic coordinates, site elevation, sampling period, and data recovery

Cluster	Site designation	Site description	Additional notes	Latitude	Longitude	Inlet Elevation(m)[a]	Data recovery (%)
Los Angeles	FRE	Urban, near freeway	∼50 m N of I-10 (West Los Angeles)	34° 04′ 11″ N	118° 09′ 02″ W	5	100
	HMS	Urban, near freeway	∼800 m E of I-10, ∼800 m N and E of I-5 curve (West Los Angeles)	34° 02′ 09″ N	118° 12′ 41″ W	12	98
	USC	Urban, near freeway	Typical urban site in downtown Los Angeles, ∼150 m W of I-110 (Central Los Angeles)	34° 01′ 09″ N	118° 16′ 38″ W	4.8	88
	CCL	Urban, community	∼1.5 km E of I-110 and ∼3.0 km S of I-10 (Central Los Angeles)	34° 00′ 23″ N	118° 17′ 59″ W	6	98
	LDS	Urban, near freeway	∼100 m W of I-405, ∼1.25 km S of I-10 (East Los Angeles)	34° 01′ 12″ N	118° 25′ 33″ W	6	94
	GRD	Urban, community	∼1.5 km W of I-405 (East Los Angeles)	33° 59′ 40″ N	118° 25′ 07″ W	6	90
Long Beach	HUD	Urban, source, near freeway	Located in the port of Los Angeles area, ∼100 m E of Terminal Island Freeway, and 1.2 km W of I-710	33° 48′ 09″ N	118° 13′ 12″ W	4	98
Riverside County	GRA	Semirural, receptor, near freeway	Semirural receptor site in the inland valley, ∼100 N of CA-60	34° 01′ 14″ N	117° 29′ 21″ W	6	88
	VBR	Semirural, receptor	Semirural receptor site, ∼3.0 km S of CA-60	33° 59′ 45″ N	117° 29′ 31″ W	4	92
Lancaster	LAN	Desert	Typical desert site away from urban sources, 2.0 km of W of CA-14	34° 40′ 09″ N	118° 07′ 51″ W	5.5	88

[a]Height relative to the ground.

2.3. Analytical Methods

The elemental composition of the CPM samples was determined by high-resolution SF-ICP-MS after dissolution of the filter-borne PM using a microwave-aided mixed-acid digestion (Lough et al. 2005; Herner et al. 2006). A mixture of 1.0 mL of 16 N HNO_3 (Optima grade, Fisher Scientific, Pittsburgh, PA, USA), 0.2 mL of 28 N HF (Ultex grade, J.T. Baker), and 0.35 mL of 12 N HCl (Optima grade, Fisher Scientific, Pittsburgh, PA, USA) was used for PM dissolution in Teflon bombs with a programmable microwave digestion unit (ETHOS, Milestone). The procedure is described in detail by Herner et al. (2006). Digestates were diluted to 15 mL with high purity water (18 MΩ/cm) and stored in low-density polyethylene (LDPE) bottles, precleaned in 2.4 N HCl for 48 h, 3.2 N HNO_3 for 48 h, and rinsed with milli-Q (Millipore, Bedford, MA, USA).

The digestates were analyzed for forty-nine elements by SF-ICPMS (Thermo-Finnigan Element 2), of which forty-two were selected, based on signal-to-noise metrics, for inclusion in the data analysis. The analytical uncertainties were determined by sum-of-squares propagation of the uncertainty of the SF-ICP-MS measurement (standard deviation of 3 replicate measurements), the uncertainty of the method blank (standard deviation of 4–5 batch specific blanks), and an estimate of the uncertainty in the digestion method and the standard deviation of replicate analyses of National Institute of Standards and Technology (NIST) Standard Reference Materials (SRMs). Six

solid samples of three SRMs were digested and analyzed with every batch of twenty-five samples. Subsequently, the total uncertainty of each measurement was determined by propagation of the analytical component (above) with the uncertainty of the field blanks. The elemental data were considered detectable if the sample value was greater than twice the estimated total uncertainty. The method detection limits (MDLs) for the quantified species are presented in Table S1.

3. RESULTS AND DISCUSSION

3.1. Temporal and Spatial Variations in CPM Mass Concentrations

A summary of CPM mass concentration data, including geometric and arithmetic means and standard deviations, is presented for each site in Tables 2–5. A detailed description of the temporal and spatial variations in CPM mass from this study was previously reported by Pakbin et al. (2010). Briefly, the annual geometric mean concentrations observed across all 10 sites were in a similar range (ca. 10 ± 2 μg/m^3), with the exception of LAN, which had a significantly lower concentration (ca. 5 μg/m^3). At most sites, summer CPM concentrations were about 2–4 times higher than winter concentrations, with the exception of the HUD site, heavily influenced by port activities in Long Beach and high heavy duty truck traffic, which had summer concentrations slightly lower than winter. The rural sites in Riverside showed the highest seasonal variations. The generally higher summer CPM concentrations were attributed to higher contributions of windblown soils and dusts to overall PM concentrations due to increased southwesterly winds (Sardar et al. 2005; Moore et al. 2010; Pakbin et al. 2010). More stable atmospheric conditions in winter, coupled with relatively lower mixing heights, result in a reduced contribution of windblown dust, thus increasing the relative contribution of vehicular traffic-induced emissions such as those from abraded brake lining and tire wear.

Most trace metal concentrations lie within the range of 0.01–10 ng/m^3, with only Na (554.5 ± 293.8 ng/m^3), Fe (312.6 ± 99.0 ng/m^3), Ca (209.7 ± 67.2 ng/m^3), Al (209.6 ± 73.1 ng/m^3), Mg (119.0 ± 41.5 ng/m^3), S (110.4 ± 43.8 ng/m^3), K (91.4 ± 31.1 ng/m^3), Ti (19.7 ± 5.8 ng/m^3), Ba (15.5 ± 5.5 ng/m^3), and Cu (13.5 ± 4.3 ng/m^3) exceeding 10 ng/m^3. The annual, winter, and summer geometric means of selected elemental concentrations (in ng/m^3) and the total CPM mass concentrations (in μg/m^3), along with their standard deviations at each site cluster, are presented in Tables 2–5, while the monthly geometric means and standard deviations of all elemental concentrations are also presented in the supplemental material (Tables S6–S9). Concentrations generally rise in the proximity of roadways, reaching values up to 10 times higher than at the rural desert site in Lancaster. The intercorrelation of selected trace elements and metals is presented in the supplemental material

TABLE 2
Los Angeles

		Annual average[a]	*SD*[b]	Winter average[c]	*SD*	Summer average[d]	*SD*
CPM Mass concentration (μg/m^3)		10.5	4.4	6.9	3.2	12.4	3.9
PC1	Al	175.2	63.6	140.5	74.9	178.5	16.1
	K	78.9	27.1	63.9	22.4	75.6	22.1
	Ca	194.3	66.6	164.3	60.1	174.3	29.3
	Ti	19.4	6.9	19.3	7.9	16.1	3.9
PC1 & PC2	Fe	322.3	139.9	392.1	125.9	217.4	20.6
PC2	Cu	16.8	6.9	23.7	6.7	12.8	1.7
	Sb	2.1	1.3	3.4	1.0	1.2	0.1
	Ba	19.2	9.6	27.0	7.9	11.6	1.3
	Pb	1.3	0.5	1.3	0.4	1.0	0.2
PC3	Zn	5.7	3.3	7.5	2.4	3.9	1.1
PC4	Cd	0.017	0.007	0.014	0.004	0.016	0.003
	Ce	0.33	0.10	0.35	0.08	0.27	0.03
PC5	S	112.7	46.0	73.7	22.4	163.9	52.3
	V	0.61	0.19	0.44	0.16	0.73	0.03
PC6	Cr	1.1	0.6	1.7	0.5	0.7	0.1
	Ni	0.6	0.2	0.7	0.1	0.4	0.1
PC7	Na	570.2	361.8	257.6	80.8	999.4	396.5
	Mg	108.3	36.8	69.2	5.1	135.1	41.7
PC8	Pt	0.003	0.001	0.003	0.001	0.002	0.001

Note: All elemental concentrations are in ng/m^3.
[a]Arithmetic mean, [b]standard deviation, [c]winter = December–February, [d]summer = June–August.

TABLE 3
Long Beach

		Annual average[a]	*SD*[b]	Winter average[c]	*SD*	Summer average[d]	*SD*
CPM Mass concentration (μg/m^3)		13.4	6.0	13.8	8.6	11.2	4.0
PC1	Al	318.9	133.9	433.0	24.8	221.1	48.4
	K	150.4	49.8	157.3	3.3	121.4	79.0
	Ca	306.1	93.1	352.7	0.2	240.9	31.5
	Ti	25.2	10.6	38.1	0.5	16.0	2.3
PC1 & PC2	Fe	394.6	210.6	576.5	23.4	240.5	38.8
PC2	Cu	9.9	6.4	19.0	2.8	5.7	2.7
	Sb	1.1	0.9	2.3	0.2	0.5	0.1
	Ba	17.5	10.4	28.9	0.7	9.8	1.3
	Pb	1.3	0.6	1.8	0.2	0.7	0.0
PC3	Zn	10.1	6.1	16.2	0.5	6.5	6.0
PC4	Cd	0.022	0.012	0.035	0.010	0.013	0.001
	Ce	0.39	0.15	0.50	0.01	0.25	0.01
PC5	S	166.0	44.1	125.0	34.4	191.4	20.5
	V	1.69	0.38	1.80	0.64	1.76	0.40
PC6	Cr	1.0	0.7	1.9	0.3	0.5	0.1
	Ni	1.3	0.6	1.4	0.5	1.0	0.2
PC7	Na	668.3	264.1	375.6	173.5	933.4	291.2
	Mg	141.4	23.6	131.4	8.0	141.2	30.3
PC8	Pt	0.002	0.003	0.005	0.004	0.002	0.005

Note: All elemental concentrations are in ng/m^3.
[a]Arithmetic mean, [b]standard deviation, [c]winter = December–February, [d]summer = June–August.

TABLE 4
Riverside

		Annual average[a]	*SD*[b]	Winter average[c]	*SD*	Summer average[d]	*SD*
CPM Mass concentration (μg/m^3)		13.5	7.9	5.7	4.1	18.7	5.6
PC1	Al	313.8	150.2	159.4	14.6	401.2	16.9
	K	159.7	83.1	66.8	6.6	258.4	17.4
	Ca	318.0	135.7	154.0	15.8	437.1	9.2
	Ti	26.0	11.2	13.3	0.7	36.1	3.5
PC1 & PC2	Fe	355.2	125.9	211.3	35.5	431.7	25.7
PC2	Cu	7.7	2.6	8.7	1.7	6.9	1.2
	Sb	1.0	0.3	0.8	0.2	1.1	0.1
	Ba	12.6	4.0	9.1	2.0	13.6	0.2
	Pb	0.8	0.3	0.5	07,	0.8	0.1
PC3	Zn	5.0	1.5	4.8	0.9	5.2	0.2
PC4	Cd	0.016	0.004	0.013	0.002	0.016	0.003
	Ce	0.39	0.11	0.31	0.13	0.42	0.02
PC5	S	86.6	54.6	43.8	11.0	156.0	38.8
	V	0.82	0.41	0.39	0.03	1.16	0.12
PC6	Cr	1.0	0.5	1.1	0.6	0.9	0.1
	Ni	0.5	0.2	0.3	0.2	0.7	0.1
PP7	Na	356.7	284.5	152.9	28.8	697.1	346.2
	Mg	124.5	65.5	49.7	8.3	198.8	36.9
PC8	Pt	0.002	0.001	0.001	0.001	0.002	0.001

Note: All elemental concentrations are in ng/m^3.
[a]Arithmetic mean, [b]standard deviation, [c]winter = December–February, [d]summer = June–August.

TABLE 5
Lancaster

		Annual average[a]	*SD*[b]	Winter average[c]	*SD*	Summer average[d]	*SD*
CPM Mass concentration (μg/m^3)		5.2	3.2	3.1	2.5	5.2	2.5
PC1	Al	184.9	272.3	57.6	28.3	353.4	362.5
	K	75.4	65.6	33.2	18.8	128.5	75.3
	Ca	129.8	157.3	46.7	18.4	226.8	226.9
	Ti	19.2	23.3	8.2	4.7	35.7	32.1
PC1 & PC2	Fe	208.4	204.6	89.3	40.6	359.7	258.7
PC2	Cu	11.7	11.4	9.4	6.0	17.9	20.8
	Sb	0.4	0.2	0.4	0.2	0.4	0.2
	Ba	6.5	4.4	4.2	1.6	8.1	5.9
	Pb	0.5	0.4	0.2	0.1	0.7	0.6
PC3	Zn	4.1	2.0	2.9	0.4	4.8	2.5
PC4	Cd	0.009	0.006	0.005	0.001	0.014	0.008
	Ce	0.26	0.27	0.13	0.08	0.32	0.33
PC5	S	46.9	33.9	23.0	11.1	81.3	32.2
	V	0.57	0.54	0.23	0.12	1.07	0.63
PC6	Cr	0.6	0.5	0.3	0.1	0.9	0.7
	Ni	0.4	0.3	0.2	0.1	0.5	0.4
PC7	Na	124.1	122.7	54.3	11.1	217.1	184.2
	Mg	51.4	66.1	17.9	3.7	91.5	92.6
PC8	Pt	0.001	0.000	0.001	0.000	0.001	0.000

Note: All elemental concentrations are in ng/m^3.
[a]Arithmetic mean, [b]standard deviation, [c]winter = December–February, [d]summer = June–August.

(Figure S2a–d), in a matrix composed of Pearson coefficients. The elements selected for presentation were chosen based upon the source apportionment analysis and data interpretation presented in the subsequent sections.

3.2. Principal Component Analysis (PCA)

To qualitatively identify the potential sources of trace metals species in CPM, PCA was employed. PCA was chosen as the receptor model, because the application of chemical mass balance (CMB) requires a detailed quantitative knowledge of the emission source profiles, currently unavailable for many of the trace element and metal species quantified in this study, whereas for PCA, qualitative knowledge of the sources is sufficient. Moreover, the source profiles may not be consistent among the different sites due to physicochemical changes of the urban aerosols with transport from source to receptor areas of the basin, which may result in differences in particle size distributions for key CPM sources. PCA was applied to a matrix composed of chemically fractionated CPM data, including only species that had signal-to-noise ratios (S/N) above unity in more than 80% of the samples (forty-two species from the total forty-nine species analyzed by SF-ICP-MS). Values below the criterion threshold (S/N < 1) were replaced by a value chosen randomly between zero and the MDL of that specific element for the statistical analysis, in order to avoid false correlations between variables with multiple below detection limit values.

In PCA, the algorithm attempts to explain the variance in a multivariate dataset with the minimum possible number of factors. If the variables are correlated with each other, a large portion of variance in the dataset can be explained with a small number of factors.

The primary PCA was applied to a pooled dataset from all the sampling sites with the exception of the Lancaster site. The Lancaster site was heavily influenced by wind-induced soil emissions from the surrounding deserts, thereby making it a unique "desert-like" site compared with the rest, and therefore PCA was performed separately for that site. The VARIMAX rotated factor matrix for the CPM metal data from all the sites (except Lancaster) is presented in Table 6 along with the factor loadings, associated eigenvalues, and variance, while the PCA results for Lancaster are presented in Table S2. The VARIMAX rotation was used to redistribute the variance to give a more interpretable structure to the factors (Henry 1987). In the tables, PCA factors are sorted in descending order of the corresponding eigenvalues. Eight components with eigenvalues greater than unity after the VARIMAX rotation were retained in the PCA, accounting for over 80% of the total variance, with roughly 34% accounted for by the first component. The elements were considered to identify the source categories when their factor loadings were larger than 0.5. Identifications of probable sources of each principal component were based primarily on the source profiles and the presence of marker species. These identifications should

TABLE 6
Principal component loadings (VARIMAX normalized) of selected trace element and metal species in airborne CPM

	Principal component							
	PC1	PC2	PC3	PC4	PC5	PC6	PC7	PC8
Dy	**0.95**	0.09	0.21	0.04	0.05	−0.04	−0.08	0.04
Rb	**0.95**	0.02	0.04	0.05	0.01	0.02	−0.10	−0.04
Cs	**0.91**	−0.01	0.26	0.04	−0.05	0.04	0.02	0.01
Nd	**0.90**	0.22	0.15	0.10	0.14	−0.02	−0.06	0.14
Ho	**0.90**	0.10	0.33	0.04	0.01	−0.03	−0.10	0.03
Yb	**0.90**	0.18	0.26	0.01	0.06	−0.01	−0.07	0.04
Y	**0.89**	0.19	0.12	0.11	0.11	−0.05	−0.01	0.03
Pr	**0.83**	0.28	0.11	0.14	0.21	−0.04	−0.05	0.20
Sm	**0.83**	0.07	0.29	0.04	0.37	−0.06	−0.09	0.11
Ca	**0.82**	0.17	0.19	0.07	0.02	0.07	0.23	0.13
Mn	**0.80**	0.44	0.15	0.12	0.04	0.10	−0.13	−0.03
Sr	**0.76**	0.47	0.09	0.08	0.06	0.09	0.15	0.00
Lu	**0.76**	0.21	0.44	0.02	−0.01	−0.07	−0.07	0.09
Ti	**0.75**	0.51	0.15	0.11	0.04	0.07	−0.14	−0.01
Li	**0.72**	0.02	−0.12	0.02	0.04	0.02	0.03	−0.12
Eu	0.64	0.48	0.04	0.05	0.08	0.03	−0.02	0.15
Al	0.62	0.10	0.01	0.02	0.05	0.01	0.05	−0.05
K	0.61	−0.06	0.03	0.06	0.00	0.14	0.10	−0.18
As	0.56	0.32	−0.06	−0.01	−0.04	0.20	0.00	−0.17
Nb	0.52	0.37	0.61	0.12	−0.06	0.19	−0.02	0.20
Fe	0.56	**0.77**	0.10	0.10	0.03	0.08	−0.11	−0.01
Sb	0.12	**0.95**	0.01	0.07	−0.05	0.05	−0.08	0.02
Ba	0.28	**0.92**	0.03	0.10	0.01	0.04	−0.09	0.01
Mo	0.10	**0.92**	0.03	0.03	0.03	0.20	−0.03	0.05
Cu	0.13	**0.83**	0.06	0.16	−0.01	0.02	0.02	−0.04
Rh	0.00	**0.78**	0.16	0.02	−0.03	0.03	0.18	0.12
Pb	0.18	0.61	−0.05	0.15	0.12	0.09	−0.06	0.16
Th	0.41	0.00	**0.86**	0.06	−0.07	−0.03	−0.01	0.09
Sc	0.48	−0.01	**0.82**	0.05	−0.05	−0.05	−0.02	0.09
W	−0.01	0.06	0.68	−0.07	0.37	0.19	0.00	−0.33
Zn	0.11	0.35	0.54	0.62	0.13	0.00	−0.09	−0.04
Cd	0.10	0.15	0.02	**0.91**	0.04	0.07	0.01	−0.06
Ce	0.24	0.22	0.01	**0.82**	0.13	0.04	0.02	0.10
La	0.13	0.04	0.00	0.10	**0.83**	−0.04	−0.01	0.29
V	0.37	−0.04	0.11	0.03	0.68	0.07	−0.04	−0.16
S	−0.18	−0.01	−0.09	0.33	0.59	0.02	0.45	−0.12
Ni	−0.02	0.08	0.01	0.06	0.03	**0.89**	0.02	0.16
Cr	0.06	0.23	0.05	0.05	0.00	**0.86**	0.01	0.04
Mg	0.39	0.01	0.03	−0.05	−0.01	0.02	**0.83**	0.10
Na	−0.41	−0.11	−0.08	0.01	0.05	0.01	**0.80**	−0.04
Pt	0.01	0.23	0.03	−0.01	0.07	0.24	0.03	**0.73**
Co	0.41	0.29	0.38	0.02	0.35	0.38	−0.07	−0.30
Eigenvalue	14.12	6.73	3.48	2.22	2.09	1.99	1.79	1.22
% of variance	33.62	16.03	8.28	5.28	4.97	4.73	4.27	2.91

Note: Loadings higher than 0.7 are shown in bold, and loadings between 0.5 and 0.7 are underlined.

not be considered definitive, as there could be some blending between the factors.

PCA was also applied to the data pooled by different site clusters (i.e., Los Angeles, Long Beach, Riverside, and Lancaster). Owing to space limitations, the results of PCA for each site cluster are not presented here, but were used in the interpretation of the results, and are presented in the supplemental material (Tables S2–S5). In general, PCA yielded consistent patterns across different site clusters, with relatively similar source profiles in sampling sites located in Los Angeles, Long Beach, and Riverside; while in Lancaster, most trace element and metal species had predictably high factor loadings in the soil-driven first principal component, accounting for 33.2% of the total variance, thus emphasizing the dominant influence of soil emissions at this site (Table S2).

With this approach, the main sources and the most representative variables were quantitatively identified. The first principal component (PC1) appears to represent soil dust, with a strong contribution from the major crustal metals such as Ca, Mn, Ti, Li, Al, K, Fe, and many of the soil source dominated rare earth elements (REEs; Dy, Nd, Ho, Yb, Y, Pr, Sm, Lu, Eu, etc.). The second principal component (PC2) has strong factor loadings for species that are considered tracers of abrasive vehicular emissions (e.g., tire and break wear), most notably Sb, Ba, Mo, Cu, Rh, Fe, and Pb.

The interpretation of the third principal component (PC3) is not as clear, partly because of the distribution of some of the PC3 factor loadings between PC3 and other components. For example, Zn factor loadings are of similar magnitude in both PC3 and the fourth principal component (PC4; and to a lower extend in PC2), while the REEs in PC3 also have high factor loadings in PC1. These species, in particular W, Sc, and Th, had higher factor loadings when PCA was applied to the data from Long Beach (Table S3) and may represent nearby industrial sources. High factor loadings of Cd and Ce in PC4 may represent plastic dust, resuspended from the debris from ground-up plastics. Both Cd and Ce are commonly used as dyeing agents in plastic production.

The fifth principal component (PC5) has high factor loadings of La, V, and S, all of which had higher factor loadings when PCA was applied to the data from Long Beach, probably representing ship emissions, particularly from the ports of Los Angeles and Long Beach. The sixth principal component (PC6) has the highest loadings for Ni and Cr. These two metal species are often associated with plating industries and abrasive vehicular emissions and had much higher factor loadings in the Long Beach site. The seventh principal component (PC7) contains most of the variability for Na and Mg, evidently representing sea salt aerosol spray transported from the Pacific Ocean. The last principal component (PC8) has high factor loadings for Pt, with considerably higher loadings in the Los Angeles site cluster, likely resulting from vehicular catalytic converter wear.

3.3. Crustal Material

The contribution of mineral dust and other crustal materials to the total CPM mass was identified mainly by the presence of elements such as Ca, Mn, Ti, Li, Al, K, and Fe, which are typical tracers of mineral materials (Watson et al. 1994; Moreno et al. 2006; Perrino et al. 2009). PC1 accounted for 33.6% of the total variance. The average concentrations of total crustal elements in CPM varied both temporally and spatially. The most abundant crustal elements found in CPM were Fe (median 312.6 $\pm$ 99.0 ng/m^3 across all the sites), Ca (209.7 $\pm$ 67.2 ng/m^3), Al (209.6 $\pm$ 73.1 ng/m^3), Mg (119.0 $\pm$ 41.5 ng/m^3), K (91.4 $\pm$ 31.1 ng/m^3), Ti (19.7 $\pm$ 5.8 ng/m^3), Mn (4.4 $\pm$ 1.4 ng/m^3), and Sr (2.5 $\pm$ 3.1 ng/m^3). The sum of the elemental concentrations of these eight elements accounted for on average 56.7% of the total CPM metal content of the forty-nine measured elements (sum of the elemental concentrations of all analyzed elements) across all the sampling sites. The temporal variations in the concentrations of selected mineral material tracers across all the sites are shown in Figure 1a–d. The highest averaged annual concentrations of Al, K, Ca, and Ti were observed in the Riverside sites with less annual variations, closely followed by HUD in Long Beach and the Los Angeles sites, while average concentrations of these species in Lancaster were much lower than those in other sampling sites. The high concentrations of these species in Lancaster during summer are due to a stronger contribution of windblown dust because of higher wind speeds. However, the normalized per PM mass concentrations of Fe, Al, K, Sr, and Ti were highest in Lancaster, followed by the Riverside site cluster, indicating a higher contribution of crustal elements to the overall CPM mass in more rural sites. Although the absolute metal concentrations (ng/m^3) represent total exposure to these species, the relative (per PM mass) metal concentrations (ng of metal/mg of CPM) provide insight into different source contributions at different geographic regions. This observation is consistent with the source apportionment analysis based on the temporal and seasonal variations in CPM mass concentrations, discussed in details by Pakbin et al. (2010), showing a higher contribution of windblown soil and dust in more rural areas. Moore et al. (2010) showed that CPM concentrations in the Lancaster site accounted for the majority of PM_{10} concentrations, because of the predominant contribution of windblown dust to overall PM concentrations.

The patterns of temporal variation in ambient concentrations of the crustal elements differed among site clusters (Figure 1a–d). The urban sites in Los Angeles and the Long Beach site showed higher concentrations of crustal metals (e.g., Al, Ca, K, Ti, Fe, Sr, and Mg) during winter, despite higher overall CPM mass concentrations in summer (Pakbin et al. 2010); crustal metal concentrations peaked in October, with continued elevated concentrations evident through January/February. The concentrations of selected crustal tracers during summer remained lower and with less temporal variation. In contrast, the rural sites in Riverside and Lancaster exhibited higher

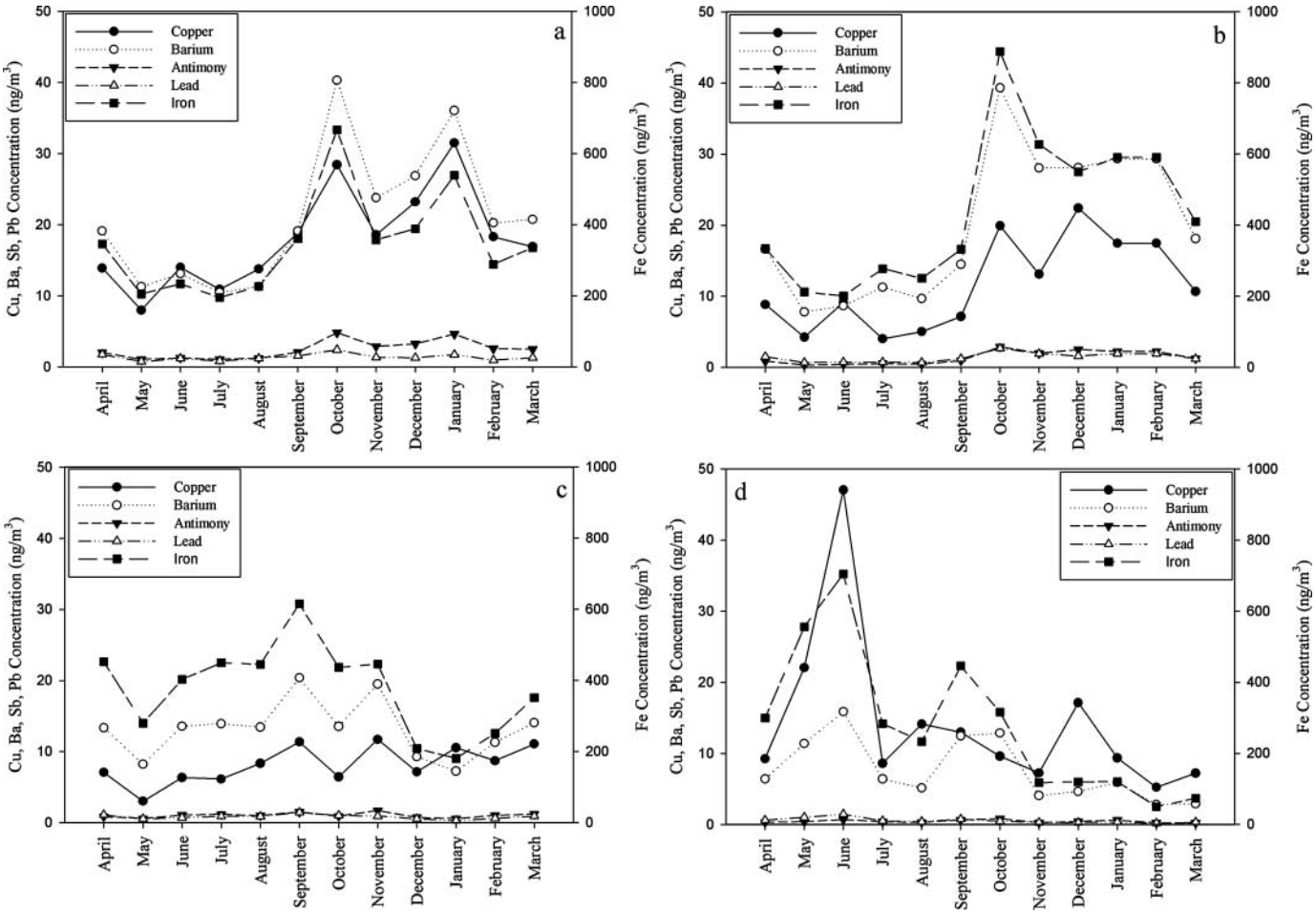

FIG. 1. Temporal variation of selected mineral dust tracers in different sampling site clusters: (a) Los Angeles cluster, (b) Long Beach, (c) Riverside cluster, and (d) Lancaster.

crustal metal contributions during summer, coupled with higher CPM mass concentrations in the same time period, thereby suggesting the higher overall contribution of windblown dust to total CPM mass in rural areas (Figure 1a–d), while in the urban sites, the contribution of traffic-induced resuspended road dust is dominating, leading to higher elemental concentrations under more stable atmospheric conditions.

3.4. Abrasive Vehicular Emissions

The second principal component (PC2) was identified as abrasive vehicular emissions, comprising trace elements such as Sb, Ba, Mo, Cu, Rh, Fe, and Pb. Among them, Sb and Ba are known as tracers of break wear (Dietl et al. 1997; Lough et al. 2005). It should be noted that Fe had a relatively high factor loading in PC1 also (0.56 compared with 0.77 in PC2, Table 6), suggesting both geologic and anthropogenic sources, also reported by Lough et al. (2005). Brake wear emissions contain significant amounts of Ba, Sb, Fe, Cu, and Zn (Garg et al. 2000) consistent with their use in brake linings; for example, Cu, Mo, Sb, and Sn are high-temperature lubricants, present in most brake linings, while Ba and Zn sulfates are commonly used as friction modifiers (Garg et al. 2000; Sternbeck et al. 2002; Sanders et al. 2003; Chan and Stachowiak 2004; Iijima et al. 2007).

Pb may be emitted from several sources, including brake wear and resuspension of road dust (Cadle et al. 1997; Garg et al. 2000; Young et al. 2002). Root (2000) demonstrated that the Pb wheel weights, widely used to balance motor vehicle wheels, which are dropped from the wheels, can be rapidly abraded and pulverized by traffic, thereby enriching the Pb content of roadway dust. High correlations between Pb concentrations and other abrasive vehicular emission tracers demonstrate that they probably have similar sources (Figure S2a–d). Although Zn had its highest factor loading in PC3 and PC4, it also had relatively high factor loadings in PC2 (Table 6). Zn is used in the form of zinc dithiophosphate in lubricating oils for gasoline vehicles as an antiwear and antioxidant additive, which may contribute to Zn emissions in CPM (Cadle et al. 1997), while Councell et al. (2004) and Fauser et al. (1999) identified Zn as a tracer for particles from tire wear.

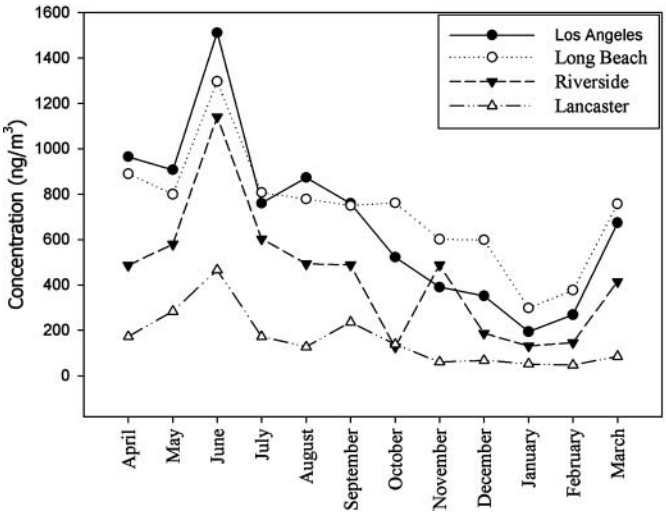

FIG. 2. Temporal variation of selected abrasive vehicular tracers in different sampling site clusters: (a) Los Angeles cluster, (b) Long Beach, (c) Riverside cluster, and (d) Lancaster.

The most abundant elements in PC2 were Fe, Ba, and Cu with an average concentration of 312.6 ± 99.0, 15.5 ± 5.5, and 13.5 ± 4.3 ng/m^3, respectively. The average CPM concentrations of Zn, Sb, Pb, Mo, and Rh were 5.7 ± 2.2, 1.6 ± 0.6, 1.0 ± 0.3, 0.4 ± 0.2 ng/m^3, and 1.13 ± 0.31 pg/m^3, respectively. Most of the elements identified in PC2 had their highest measured concentrations at the Los Angeles sites, followed by Long Beach, Riverside, and Lancaster site clusters, a trend that parallels vehicular traffic volume and reinforces a likely dominant vehicular source for these elements. Cu, Sb, Ba, and Pb concentrations were highest at the Los Angeles site cluster (16.8 ± 6.9, 2.1 ± 1.3, 19.2 ± 9.6, and 1.3 ± 0.5 ng/m^3, respectively), while Fe and Zn concentrations were higher in Long Beach (374.2 ± 207.7 and 9.9 ± 5.9 ng/m^3, respectively), probably due to additional contribution from nonabrasive vehicular emissions in Long Beach (e.g., local industrial sources). The temporal variations in ambient concentrations of selected brake wear markers across all the sites are presented in Figure 2a–d. The elemental concentrations of these metal species were highest during fall at all the sites (with higher concentrations extending into the winter in the urban sites), with the exception of Lancaster, with the highest deviations observed in the urban sites of Los Angeles between seasons, most likely due to relatively more stable atmospheric conditions that accentuates the contribution of vehicle-induced resuspended road dust.

A number of studies have reported the Cu/Sb ratio as a characteristic index of break wear; however, different values in the range of 4–12 were reported in different urban environments (Weckwerth 2001; Sternbeck et al. 2002; Furuta et al. 2005; Gomez et al. 2005; Canepari et al. 2008). Although this ratio can be dependent on the composition of the brake lining used in the studied area, our data show very little variation in the Cu/Sb ratio among all the site clusters—with the exception of Lancaster, the Cu/Sb ratio was on average (8.3 ± 0.8). The Cu/Sb ratio in Lancaster was much higher (27.3), possibly because Cu may have other sources than abraded brake wear in this area. At the Lancaster site, Cu has a high factor loading in PC1 (Table S2; along with crustal materials) and also exhibits good correlations with soil tracers (Figure S2d), further confirming this hypothesis. The Cu/Sb ratio in Long Beach (9.2) was relatively higher than Los Angeles (7.6) and Riverside (7.9), probably due to higher brake wear emissions resulting from stronger abrasion processes of heavy duty vehicles in the I-710 freeway near the sampling site.

3.5. Other Sources of CPM-Bound Metals and Trace Elements

The highest elemental factor loadings in the PC3 correspond to Th, Sc, W, Zn, and Nb (Table 6). The REEs present in PC3 (Th, Sc, Nb, and Lu) also have high factor loadings in PC1, suggesting geological origins. However, refineries and oil-fired plants are also major sources of REEs, from the widely used zeolite cracking catalysts (Olmez and Gordon 1985). An estimated 2000 tons of catalyst material is lost per day by US oil refineries (Fox 1985). Sc has application in oil refineries as a tracing agent, while Th, W, and Zn have various industrial sources, most notably industrial catalytic converters (Haynes 2010–2011). These metals generally have higher factor loadings when PCA is carried out on the data from Long Beach (Table S3), coupled with higher average concentrations, both indicative of their industrial origins in this region in proximity to multiple oil refineries; while these metals may have geologic origins in other regions. PC4 has the highest factor loadings for Cd and Ce (in addition to Zn with relatively lower factor loading), two trace metals commonly used in the dyeing process of plastics, which may be enriched and accumulated in soil and road dust over time. The spatial variations of these two species

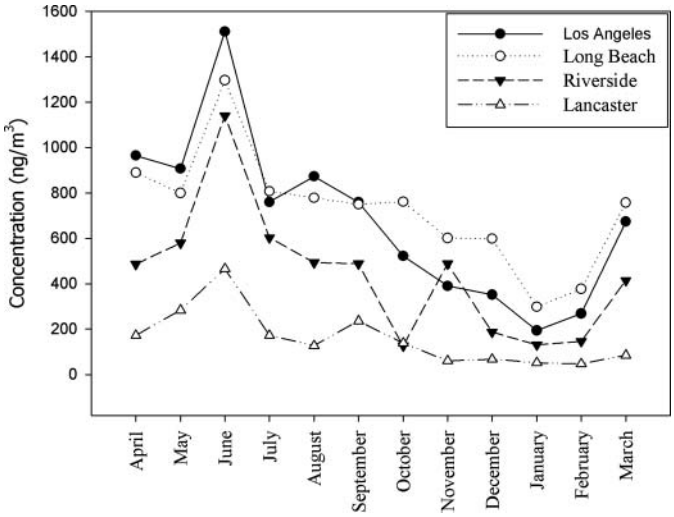

FIG. 3. Annual variation of sodium (Na), a sea salt tracer, across all the sampling sites.

were quite low across the sampling sites, with the exception of relatively higher concentrations of Cd in Lancaster. PC5 has the highest factor loadings for La, V, and S. Both V and S are known to be tracers of ship emissions (Arhami et al. 2009), which are predominantly in the fine PM size range and their presence in CPM may reflect a "tail" in the upper size distribution range; for example, S may be in the form of ammonium sulfate, which is mostly in the $PM_{2.5}$ size range (Seinfeld and Pandis 2006; Cheung et al. 2010). The presence of La in this principal component may also suggest the contribution of oil refinery emissions.

PC6 has high factor loadings for the two trace metals Ni and Cr, both often identified as markers of industrial emissions, particularly the plating industries in Los Angeles. Singh et al. (2002) attributed Ni and Cr to emissions from power plants and refineries in Long Beach, whereas Querol et al. (2007) identified Ni and V as markers of petrochemical emissions in Spanish cities, while As, Cd, Cr, Cs, Cu, Mn, Mo, Ni, and Zn were markers of different forms of metallurgy. When PCA was applied to the Long Beach data, one of the main factors (PC2) was characterized by high loadings of Cu, Cd, Cr, Mo, and Ni, along with some of the abrasive vehicular tracers (Fe, Sb, Ba, and Pb) and platinum group (Pt and Rh; Table S3), suggesting that the emissions of these elements are most likely related to the activities of the ports of Long Beach and Los Angeles as well as the heavy duty diesel truck traffic associated with these ports and their transport activities.

Marine aerosols play an important role in the overall PM composition in Los Angeles, due to the geographic orientation of the city, its proximity to the Pacific Ocean, and the prevailing westerly wind patterns. The elements with the highest loading on PC7 were Na and Mg, and this component was identified as sea spray aerosols. The PCA estimated that the marine contribution explains 4.2% of the total variance (Table 6). Na concentrations notably decreased from the coastal to the inland sites (Figure 3), with the highest concentrations observed in Long Beach (681.5 ± 253.4 ng/m^3), followed by Los Angeles sites

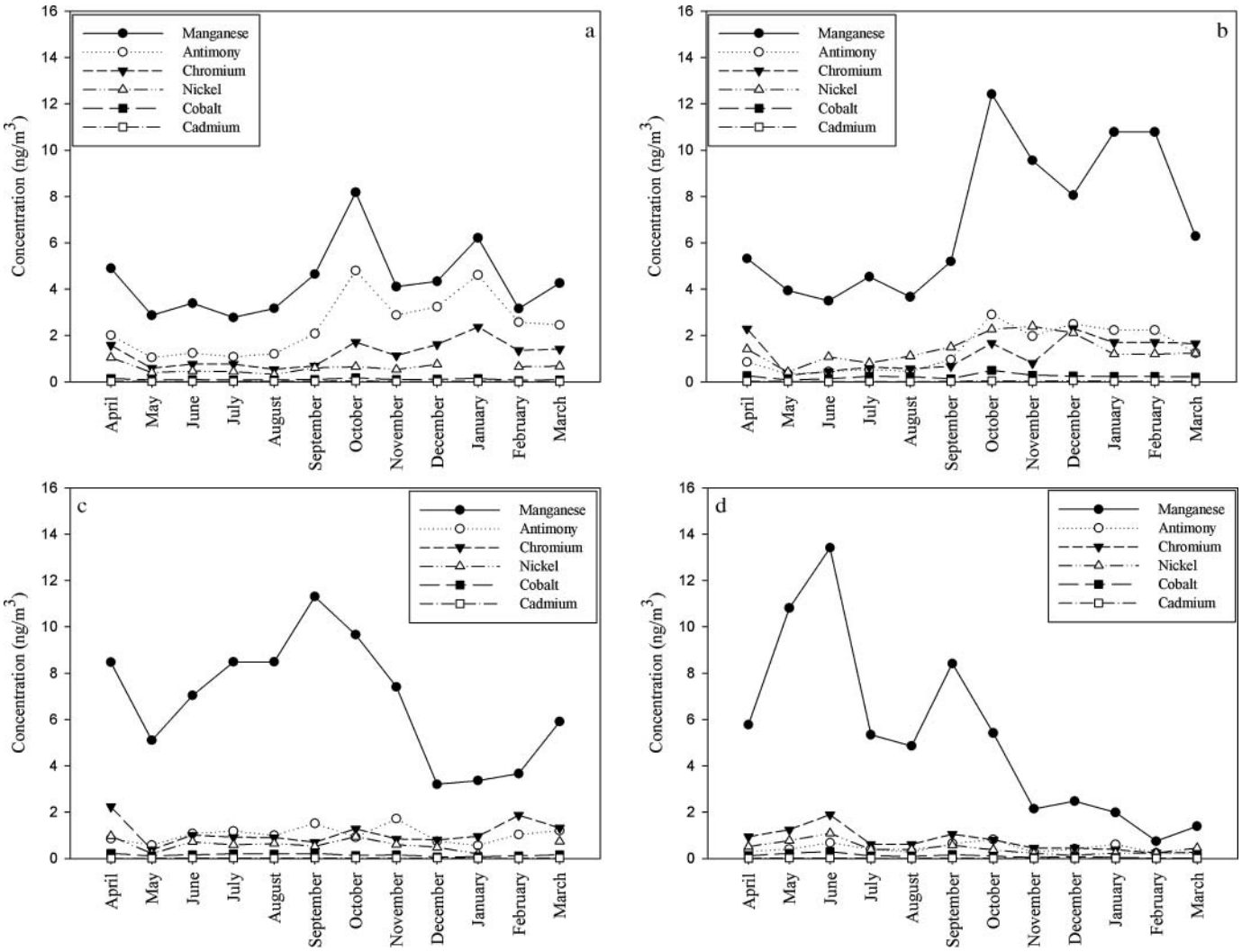

FIG. 4. Annual variation of trace metals listed as air pollutants by the US EPA: (a) Los Angeles cluster, (b) Long Beach, (c) Riverside cluster, and (d) Lancaster.

(570.2 ± 361.8 ng/m^3), Riverside sites (356.7 ± 284.5 ng/m^3), and Lancaster (124.1 ± 122.7 ng/m^3). Within the Los Angeles site cluster, the western Los Angeles sites had higher average concentrations of both Na and Mg (716.6 ± 423.7 ng/m^3). Figure 3 shows the temporal variation in the concentrations of Na across all the site clusters. The spatial variation in Mg concentrations is negligible compared with Na, with relatively higher concentrations observed in Riverside compared with Los Angeles. Mg is also a tracer of mineral dust as well as sea spray, which explains the relatively high factor loadings in both PC1 (associated to mineral dust) and PC7 (associated with sea spray).

PGEs, particularly Pt, Pd, and Rh, are widely used in automobile catalytic converters. A number of studies have linked airborne PGE concentrations to emissions resulting from chemical, physical, and thermal stresses due to mechanical abrasion and high temperatures (Rauch et al. 2001; Zereini et al. 2001; Gomez et al. 2002; Wiseman and Zereini 2009), while other studies showed an increase in PGE levels in urban soils and dusts (Whiteley and Murray 2003; Zereini et al. 1997, 2007). The average annual CPM concentrations of Pt and Rh were 2.27 (± 0.74) and 1.13 (± 0.31) pg/m^3, respectively, while Pd concentrations were below detection limits. Pt and Rh concentrations were highest in the Los Angeles site cluster, followed by Long Beach and rural sites, with the lowest concentrations observed in Lancaster. These concentrations are lower than those reported by Rauch et al. (2005) in Boston (9.4 and 2.2 pg/m^3 for Pt and Rh, respectively). In the PCA, Pt had high factor loadings in PC8, while the highest factor loading of Rh was observed in PC2. When PCA was applied to the data from the sites in each cluster separately, both Pt and Rh were in PC2 in Long Beach, along with abrasive vehicular and industrial markers (Table S3). This may be the result of higher industrial activity in the area of

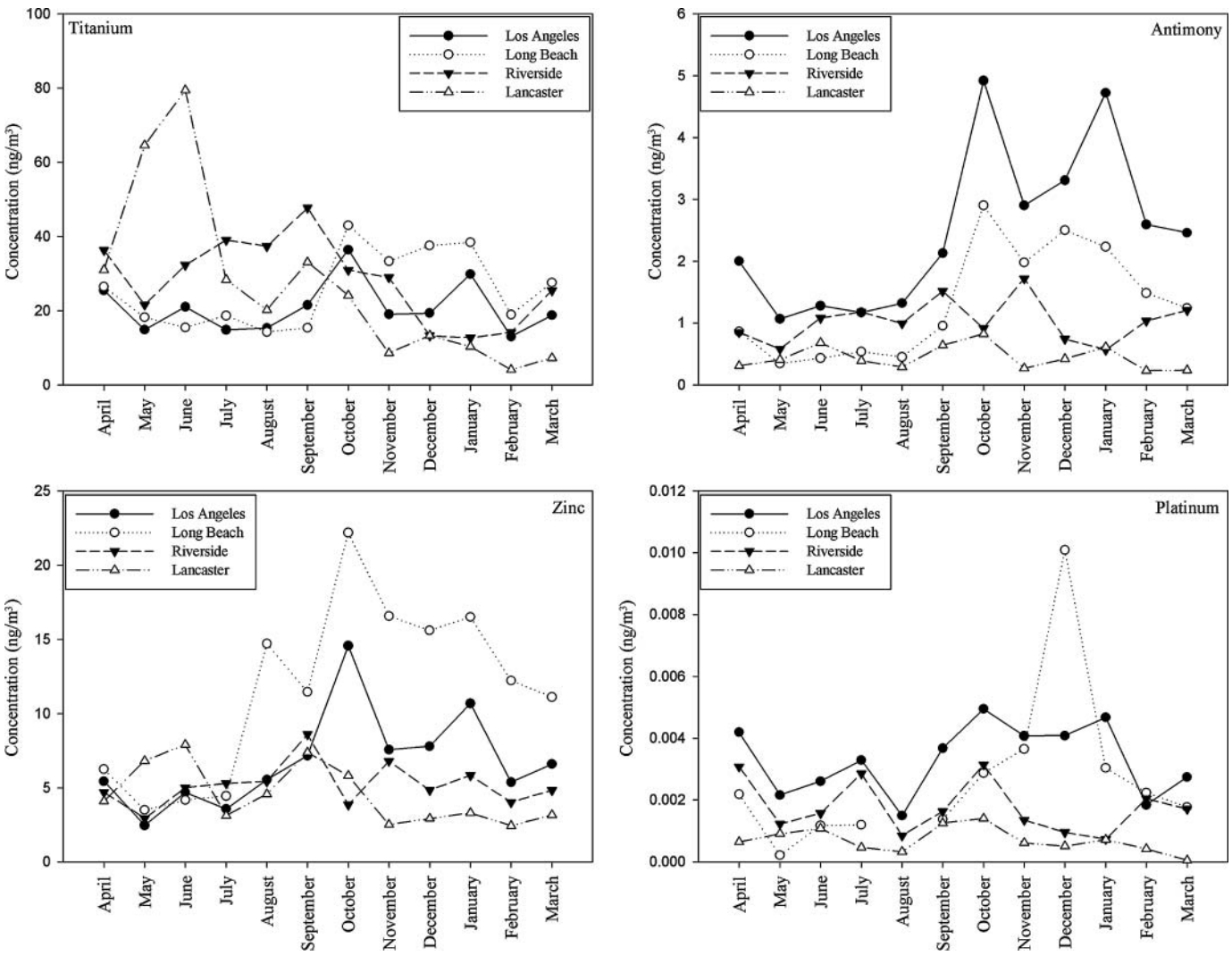

FIG. 5. Annual variation of selected metal species from the identified sources using PCA across all the sampling sites (annual variation of sea salt tracer, sodium (Na), is presented in Figure 3): (a) Titanium (Ti), (b) Antimoy (Sb), (c) Zinc (Zn), and (d) Platinum (Pt).

Long Beach and/or a higher rate of road dust resuspension due to heavy duty vehicle traffic.

Among the metal species discussed, some are reported by the US EPA as hazardous air pollutants. These elements are Sb, Be, As, Cd, Cr, Co, Pb, Mn, Hg, Ni, and Se; among which Hg was not detectable by ICP-MS methodology, while Be and Se concentrations were below the detection limit in more than 80% of the collected samples and therefore not reported. The average concentrations of these elements across all the sites were Sb (1.58 ± 0.64 ng/m^3), As (0.079 ± 0.022 ng/m^3), Cd (0.016 ± 0.005 ng/m^3), Cr (1.06 ± 0.41 ng/m^3), Co (0.11 ± 0.03 ng/m^3), Pb (1.03 ± 0.29 ng/m^3), Mn (4.36 ± 1.43 ng/m^3), and Ni (0.64 ± 0.16 ng/m^3). The temporal variations in CPM concentrations of these elements in each site cluster are presented in Figure 4a–d. With the exception of Mn, these species generally had higher concentrations in the urban sites of Los Angeles and Long Beach, with elevated concentrations throughout fall/winter, suggesting anthropogenic sources.

4. SUMMARY AND CONCLUSIONS

The samples of CPM from a year-long measurement campaign at 10 sites in the greater Los Angeles area, subject to various aerosol/pollution sources, were quantified for their element content. The PCA was applied in order to help identify CPM sources in the study area. The PCA revealed a suite of identifiable CPM sources that were consistent with data available in the literature, but also identified additional elemental markers for some of these CPM sources that are reported here for the first time. In general, trace metals associated with airborne mineral dust dominated the overall CPM mass (mainly Al, Ca, Fe, K, Mg, and Ti), while abrasive vehicular emission tracers (Fe, Ba, and Cu) also contributed significantly. Other identified CPM sources were industrial emissions, sea salt spray, and catalytic converter emissions. Each of these classes of CPM trace element and metal markers had their distinct temporal and spatial variations. Figure 5a–d shows the temporal variation of selected trace elements from each identified source, across all the site clusters. Elements in the same class had generally similar spatial variation patterns across the sites.

So far only eleven metal species have been listed in EPA as airborne toxics, while many more may induce hazardous outcomes in human health. Heavy metals accumulate in road dust as a result of atmospheric deposition and can subsequently become airborne by wind- or traffic-induced turbulence. The accumulation of heavy metals is more rapid in dry locations, such as the greater Los Angeles area, with about only 30 cm of annual precipitation on average (National Oceanic and Atmospheric Administration, NOAA). These species can also pollute urban water runoffs and/or bioaccumulate in plants. In this study, we provided a detailed description of the temporal and spatial variations of the CPM metal content in the greater Los Angeles area, linked trace element and metal species to their potential sources, and identified additional potential markers for rural and urban CPM sources. We believe that this information will help the US EPA as well as state regulatory agencies to develop and implement cost-effective strategies to protect the public from exposure to toxic compounds of CPM.

REFERENCES

Amato, F., Pandolfi, M., Escrig, A., Querol, X., Alastuey, A., Pey, J., Perez, N., and Hopke, P. K. (2009). Quantifying Road Dust Resuspension in Urban Environment by Multilinear Engine: A Comparison with PMF2. *Atmos. Environ.* 43:2770–2780.

Arhami, M., Sillanpaa, M., Hu, S. H., Olson, M. R., Schauer, J. J., and Sioutas, C. (2009). Size-Segregated Inorganic and Organic Components of PM in the Communities of the Los Angeles Harbor. *Aerosol. Sci. Tech.* 43: 145–160.

Becker, S., Dailey, L. A., Soukup, J. M., Grambow, S. C., Devlin, R. B., and Huang, Y. C. T. (2005). Seasonal Variations in Air Pollution Particle-Induced Inflammatory Mediator Release and Oxidative Stress. *Environ. Health Persp.* 113:1032–1038.

Cadle, S. H., Mulawa, P. A., Ball, J., Donase, C., Weibel, A., Sagebiel, J. C., Knapp, K. T., and Snow, R. (1997). Particulate Emission Rates from In Use High Emitting Vehicles Recruited in Orange County, California. *Environ. Sci. Technol.* 31:3405–3412.

Canepari, S., Perrino, C., Olivieri, F., and Astolfi, M. L. (2008). Characterisation of the Traffic Sources of PM through Size-Segregated Sampling, Sequential Leaching and ICP Analysis. *Atmos. Environ.* 42:8161–8175.

Canepari, S., Pietrodangelo, A., Perrino, C., Astolfi, M. L., and Marzo, M. L. (2009). Enhancement of Source Traceability of Atmospheric PM by Elemental Chemical Fractionation. *Atmos. Environ.* 43:4754–4765.

Chan, D., and Stachowiak, G. W. (2004). Review of Automotive Brake Friction Materials. *P. I. Mech. Eng. D.-J. Aut.* 218:953–966.

Cheung, K. L., Daher, N., Kam, W., Shafer, M., Ning, Z., Schauer, J. J., and Sioutas, C. (2010). Spatial and Temporal Variation of Chemical Composition and Mass Closure of Ambient Coarse Particulate Matter (PM10–2.5) in the Los Angeles Area. *Atmos. Environ.* DOI: 10.1016/j.atmosenv.2011.02.066. accepted.

Claiborn, C. S., Larson, T., and Sheppard, L. (2002). Testing the Metals Hypothesis in Spokane, Washington. *Environ. Health Persp.* 110:547–552.

Colombo, C., Monhemius, A. J., and Plant, J. A. (2008). Platinum, Palladium and Rhodium Release from Vehicle Exhaust Catalysts and Road Dust Exposed to Simulated Lung Fluids. *Ecotox. Environ. Safe* 71:722–730.

Councell, T. B., Duckenfield, K. U., Landa, E. R., and Callender, E. (2004). Tire-Wear Particles as a Source of Zinc to the Environment. *Environ. Sci. Technol.* 38:4206–4214.

Dietl, C., Reifenhauser, W., and Peichl, L. (1997). Association of Antimony with Traffic—Occurrence in Airborne Dust, Deposition and Accumulation in Standardized Grass Cultures. *Sci. Total Environ.* 205:235–244.

Fauser, P., Tjell, J. C., Mosbaek, H., and Pilegaard, K. (1999). Quantification of Tire-Tread Particles Using Extractable Organic Zinc as Tracer. *Rubber Chem. Technol.* 72:969–977.

Fox, J. L. (1985). Zeolites Catalyze Patent Dispute. *Science*, 227:35–36.

Furuta, N., Iijima, A., Kambe, A., Sakai, K., and Sato, K. (2005). Concentrations, Enrichment and Predominant Sources of Sb and Other Trace Elements in Size Classified Airborne Particulate Matter Collected in Tokyo from 1995 to 2004. *J. Environ. Monitor.* 7:1155–1161.

Gandhi, H. S., Graham, G. W., and McCabe, R. W. (2003). Automotive Exhaust Catalysis. *J. Catal.* 216:433–442.

Garg, B. D., Cadle, S. H., Mulawa, P. A., Groblicki, P. J., Laroo, C., and Parr, G. A. (2000). Brake Wear Particulate Matter Emissions. *Environ. Sci. Technol.*, 34:4463–4469.

Gavett, S. H., and Koren, H. S. (2001). The Role of Particulate Matter in Exacerbation of Atopic Asthma. *Int. Arch. Allergy Imm.* 124:109–112.

Gomez, B., Palacios, M. A., Gomez, M., Sanchez, J. L., Morrison, G., Rauch, S., McLeod, C., Ma, R., Caroli, S., Alimonti, A., Petrucci, F., Bocca, B.,

Schramel, P., Zischka, M., Petterson, C., and Wass, U. (2002). Levels and Risk Assessment for Humans and Ecosystems of Platinum-Group Elements in the Airborne Particles and Road Dust of Some European Cities. *Sci. Total Environ.* 299:1–19.

Gomez, D. R., Gine, M. F., Bellato, A. C. S., and Smichowski, P. (2005). Antimony: A Traffic-Related Element in the Atmosphere of Buenos Aires, Argentina. *J. Environ. Monitor.* 7:1162–1168.

Harrison, R. M., Yin, J. X., Mark, D., Stedman, J., Appleby, R. S., Booker, J., and Moorcroft, S. (2001). Studies of the Coarse Particle (2.5–10 μm) Component in UK Urban Atmospheres. *Atmos. Environ.* 35:3667–3679.

Haynes, W. M. (2010–2011). CRC Handbook of Chemistry and Physics, in *CRC Handbook of Chemistry and Physics*, 79th ed. W. M. Haynes, ed., CRC Press, 2610 p.

Henry, R. C. (1987). Current Factor-Analysis Receptor Models Are Ill-Posed. *Atmos. Environ.* 21:1815–1820.

Herner, J. D., Green, P. G., and Kleeman, M. J. (2006). Measuring the Trace Elemental Composition of Size-Resolved Airborne Particles. *Environ. Sci. Technol.* 40:1925–1933.

Hornberg, C., Maciuleviciute, L., Seemayer, N. H., and Kainka, E. (1998). Induction of Sister Chromatid Exchanges (SCE) in Human Tracheal Epithelial Cells by the Fractions PM-10 and PM-2.5 of Airborne Particulates. *Toxicol. Lett.*, 96–97:215–220.

Iijima, A., Sato, K., Yano, K., Tago, H., Kato, M., Kimura, H., and Furuta, N. (2007). Particle Size and Composition Distribution Analysis of Automotive Brake Abrasion Dusts for the Evaluation of Antimony Sources of Airborne Particulate Matter. *Atmos. Environ.* 41:4908–4919.

Kleinman, M. T., Sioutas, C., Chang, M. C., Boere, A. J. F., and Cassee, F. R. (2003). Ambient Fine and Coarse Particle Suppression of Alveolar Macrophage Functions. *Toxicol. Lett.* 137:151–158.

Lighty, J. S., Veranth, J. M., and Sarofim, A. F. (2000). Combustion Aerosols: Factors Governing Their Size and Composition and Implications to Human Health. *J. Air Waste Manage.* 50:1565–1618.

Lipsett, M. J., Tsai, F. C., Roger, L., Woo, M., and Ostro, B. D. (2006). Coarse Particles and Heart Rate Variability among Older Adults with Coronary Artery Disease in the Coachella Valley, California. *Environ. Health Persp.* 114:1215–1220.

Lough, G. C., Schauer, J. J., Park, J. S., Shafer, M. M., Deminter, J. T., and Weinstein, J. P. (2005). Emissions of Metals Associated with Motor Vehicle Roadways. *Environ. Sci. Technol.* 39:826–836.

Luttinger, D., and Wilson, L. (2003). A Study of Air Pollutants and Acute Asthma Exacerbations in Urban Areas: Status Report. *Environ. Pollut.* 123:399–402.

Misra, C., Geller, M. D., Sioutas, C., and Solomon, P. A. (2003). Development and Evaluation of a PM10 Impactor-Inlet for a Continuous Coarse Particle Monitor. *Aerosol. Sci. Tech.* 37:271–281.

Misra, C., Singh, M., Shen, S., Sioutas, C., and Hall, P. A. (2002). Development and Evaluation of a Personal Cascade Impactor Sampler (PCIS). *J. Aerosol. Sci.* 33:1027–1047.

Monn, C., and Becker, S. (1999). Cytotoxicity and Induction of Proinflammatory Cytokines from Human Monocytes Exposed to Fine (PM2.5) and Coarse Particles (PM10–2.5) in Outdoor and Indoor Air. *Toxicol. Appl. Pharm.* 155:245–252.

Moore, K. F., Verma, V., Minguillon, M. C., and Sioutas, C. (2010). Inter- and Intra-Community Variability in Continuous Coarse Particulate Matter (PM10–2.5) Concentrations in the Los Angeles Area. *Aerosol. Sci. Tech.* 44:526–540.

Morcelli, C. P. R., Figueiredo, A. M. G., Sarkis, J. E. S., Enzweiler, J., Kakazu, M., and Sigolo, J. B. (2005). PGEs and Other Traffic-Related Elements in Roadside Soils from Sao Paulo, Brazil. *Sci. Total Environ.* 345:81–91.

Moreno, T., Querol, X., Alastuey, A., Viana, M., Salvador, P., de la Campa, A. S., Artinano, B., de la Rosa, J., and Gibbons, W. (2006). Variations in Atmospheric PM Trace Metal Content in Spanish Towns: Illustrating the Chemical Complexity of the Inorganic Urban Aerosol Cocktail. *Atmos. Environ.* 40:6791–6803.

Olmez, I., and Gordon, G. E. (1985). Rare-Earths—Atmospheric Signatures for Oil-Fired Power-Plants and Refineries. *Science* 229:966–968.

Pakbin, P., Hudda, N., Cheung, K. L., Moore, K. F., and Sioutas, C. (2010). Spatial and Temporal Variability of Coarse (PM10–2.5) Particulate Matter Concentrations in the Los Angeles Area. *Aerosol. Sci. Tech.* 44:514–525.

Perrino, C., Canepari, S., Catrambone, M., Torre, S. D., Rantica, E., and Sargolini, T. (2009). Influence of Natural Events on the Concentration and Composition of Atmospheric Particulate Matter. *Atmos. Environ.* 43:4766–4779.

Querol, X., Viana, M., Alastuey, A., Amato, F., Moreno, T., Castillo, S., Pey, J., de la Rosa, J., de la Campa, A. S., Artinano, B., Salvador, P., Dos Santos, S. G., Fernandez-Patier, R., Moreno-Grau, S., Negral, L., Minguillon, M. C., Monfort, E., Gil, J. I., Inza, A., Ortega, L. A., Santamaria, J. M., and Zabalza, J. (2007). Source Origin of Trace Elements in PM from Regional Background, Urban and Industrial Sites of Spain. *Atmos. Environ.* 41:7219–7231.

Rauch, S., Hemond, H. F., Barbante, C., Owari, M., Morrison, G. M., Peucker-Ehrenbrink, B., and Wass, U. (2005). Importance of Automobile Exhaust Catalyst Emissions for the Depostion of Platinum, Palladium, and Rhodium in the Northern Hemisphere. *Environ. Sci. Technol.* 39:8156–8162.

Rauch, S., Lu, M., and Morrison, G. M. (2001). Heterogeneity of Platinum Group Metals in Airborne Particles. *Environ. Sci. Technol.* 35:595–599.

Root, R. A. (2000). Lead Loading of Urban Streets by Motor Vehicle Wheel Weights. *Environ. Health Persp.* 108:937–940.

Sanders, P. G., Xu, N., Dalka, T. M., and Maricq, M. M. (2003). Airborne Brake Wear Debris: Size Distributions, Composition, and a Comparison of Dynamometer and Vehicle Tests. *Environ. Sci. Technol.* 37:4060–4069.

Sardar, S. B., Fine, P. M., and Sioutas, C. (2005). Seasonal and Spatial Variability of the Size-Resolved Chemical Composition of Particulate Matter (PM10) in the Los Angeles Basin. *Journal of Geophysical Research* 110:D07508.

Seinfeld, J. H., and Pandis, S. N. (2006). *Atmospheric Chemistry and Physics—From Air Pollution to Climate Change.* John Wiley & Sons.

Singh, M., Jaques, P. A., and Sioutas, C. (2002). Size Distribution and Diurnal Characteristics of Particle-Bound Metals in Source and Receptor Sites of the Los Angeles Basin. *Atmos. Environ.* 36:1675–1689.

Singh, M., Misra, C., and Sioutas, C. (2003). Field Evaluation of a Personal Cascade Impactor Sampler (PCIS). *Atmos. Environ.* 37:4781–4793.

Smith, K. R., and Aust, A. E. (1997). Mobilization of Iron from Urban Particulates Leads to Generation of Reactive Oxygen Species In Vitro and Induction of Ferritin Synthesis in Human Lung Epithelial Cells. *Chem. Res. Toxicol.* 10:828–834.

Sternbeck, J., Sjodin, A., and Andreasson, K. (2002). Metal Emissions from Road Traffic and the Influence of Resuspension—Results from Two Tunnel Studies. *Atmos. Environ.* 36:4735–4744.

Thorpe, A., and Harrison, R. M. (2008). Sources and Properties of Non-Exhaust Particulate Matter from Road Traffic: A Review. *Sci. Total Environ.* 400:270–282.

Tsai, F. C., Apte, M. G., and Daisey, J. M. (2000). An Exploratory Analysis of the Relationship between Mortality and the Chemical Composition of Airborne Particulate Matter. *Inhal. Toxicol.* 12:121–135.

Villeneuve, P. J., Burnett, R. T., Shi, Y. L., Krewski, D., Goldberg, M. S., Hertzman, C., Chen, Y., and Brook, J. (2003). A Time-Series Study of Air Pollution, Socioeconomic Status, and Mortality in Vancouver, Canada. *J. Expo. Anal. Env. Epid.* 13:427–435.

Watson, J. G., Chow, J. C., Lu, Z. Q., Fujita, E. M., Lowenthal, D. H., Lawson, D. R., and Ashbaugh, L. L. (1994). Chemical Mass-Balance Source Apportionment of PM(10) during the Southern California Air-Quality Study. *Aerosol. Sci. Tech.* 21:1–36.

Weckwerth, G. (2001). Verification of Traffic Emitted Aerosol Components in the Ambient Air of Cologne (Germany). *Atmos. Environ.* 35:5525–5536.

Whiteley, J. D., and Murray, F. (2003). Anthropogenic Platinum Group Element (Pt, Pd and Rh) Concentrations in Road Dusts and Roadside Soils from Perth, Western Australia. *Sci. Total Environ.* 317:121–135.

Wiseman, C. L. S., and Zereini, F. (2009). Airborne Particulate Matter, Platinum Group Elements and Human Health: A Review of Recent Evidence. *Sci. Total Environ.* 407:2493–2500.

Yeatts, K., Svendsen, E., Creason, J., Alexis, N., Herbst, M., Scott, J., Kupper, L., Williams, R., Neas, L., Cascio, W., Devlin, R. B., and Peden, D. B. (2007). Coarse Particulate Matter (PM2.5–10) Affects Heart Rate Variability, Blood Lipids, and Circulating Eosinophils in Adults with Asthma. *Environ. Health Persp.* 115:709–714.

Young, T. M., Heeraman, D. A., Sirin, G., and Ashbaugh, L. L. (2002). Resuspension of Soil as a Source of Airborne Lead near Industrial Facilities and Highways. *Environ. Sci. Technol.* 36:2484–2490.

Zereini, F., Skerstupp, B., Alt, F., Helmers, E., and Urban, H. (1997). Geochemical Behaviour of Platinum-Group Elements (PGE) in Particulate Emissions by Automobile Exhaust Catalysts: Experimental Results and Environmental Investigations. *Sci. Total Environ.* 206:137–146.

Zereini, F., Wiseman, C., Alt, F., Messerschmidt, J., Muller, J., and Urban, H. (2001). Platinum and Rhodium Concentrations in Airborne Particulate Matter in Germany from 1988 to 1998. *Environ. Sci. Technol.* 35:1996–2000.

Zereini, F., Wiseman, C., and Puttmann, W. (2007). Changes in Palladium, Platinum, and Rhodium Concentrations, and Their Spatial Distribution in Soils along a Major Highway in Germany from 1994 to 2004. *Environ. Sci. Technol.* 41:451–456.